Impurity center in a semiconductor quantum ring in the presence of a radial electric field

Boris S. Monozon,[1,*] Mikhail V. Ivanov,[2,†] and Peter Schmelcher[2,3,‡]
[1]*Physics Department, Marine Technical University, 3 Lotsmanskaya Street, 190008 St. Petersburg, Russia*
[2]*Theoretische Chemie, Institut für Physikalische Chemie, Universität Heidelberg, INF 229, 69120 Heidelberg, Germany*
[3]*Physikalisches Institut, Universität Heidelberg, Philosophenweg 12, 69120 Heidelberg, Germany*
(Received 12 March 2004; revised manuscript received 17 September 2004; published 23 November 2004)

The problem of an impurity electron in a quantum ring (QR) in the presence of a radially directed strong external electric field is investigated in detail. Both an analytical and a numerical approach to the problem are developed. The analytical investigation focuses on the regime of a strong wire-electric field compared to the electric field due to the impurity. An adiabatic and quasiclassical approximation is employed. The explicit dependences of the binding energy of the impurity electron on the electric field strength, parameters of the QR, and position of the impurity within the QR are obtained. Numerical calculations of the binding energy based on a finite-difference method in two and three dimensions are performed for arbitrary strengths of the electric field. It is shown that the binding energy of the impurity electron exhibits a maximum as a function of the radial position of the impurity that can be shifted arbitrarily by applying a corresponding wire-electric field. The maximal binding energy monotonically increases with increasing electric field strength. The inversion effect of the electric field is found to occur. An increase of the longitudinal displacement of the impurity typically leads to a decrease of the binding energy. Results for both low- and high-quantum rings are derived and discussed. Suggestions for an experimentally accessible setup associated with the GaAs/GaAlAs QR are provided.

DOI: 10.1103/PhysRevB.70.205336 PACS number(s): 73.21.−b, 78.20.Bh, 73.20.Hb

I. INTRODUCTION

During the last decade electronic and optical properties of low-dimensional semiconductor structures have been studied extensively both experimentally and theoretically. Along with long-known systems like quantum wells, quantum wires, quantum dots, and superlattices, the novel confined structures called quantum rings (QR's) attract much attention. The QR can be viewed as a cylindrical quantum dot consisting of an axially symmetric cavity. The unique topology of the QR leads to remarkable quantum phenomena. In the presence of an axially directed magnetic field persistent current and oscillations of the electron energy as a function of the magnetic flux (Aharonov-Bohm effect) were found to occur.[1]

It is common knowledge that impurities and/or excitons modify considerably the electronic, optical, and kinetic properties of low-dimensional structures such as QR's. Also these properties are strongly affected by external magnetic and electric fields. Today, an extensive literature is available which traces the effects of a magnetic field on free carriers, excitons, and impurity states in the QR (see, for example, Lin and Guo[2] and Monozon and Schmelcher[3] and references therein). At the same time the influence of an electric field on the electronic properties of a QR has attracted much less attention. The energy levels of free electrons and the oscillator strengths of the interband optical transitions as a function of the radii of the QR and strength of the in-plane electric field were investigated in Ref. 4. Barticevic *et al.*[5] studied theoretically the effect of the in-plane electric field on the Aharonov-Bohm oscillations and the optical absorption in the QR in the absence of impurities and excitons. The effects of the eccentricity and an in-plane electric field on the electronic and optical properties of elliptical QR's have been considered in Ref. 6. Recently the influence of the in-plane electric field on the persistent current in the QR coupled to a quantum wire was studied.[7] In contrast to Refs. 4–7 the effect of the impurity center on the electronic states in the QR subject to an axially directed magnetic and radially directed electric fields was taken into account in Ref. 3. The influence of the radial electric field on the electron was assumed to be much weaker than that of the impurity center, magnetic field, and confinement. However, the influence of a strong electric field on the impurity states in the QR is certainly of interest. The reason for this is that a strong electric field induces a considerable polarization of the spatial distribution of the carriers.[4,6] Note that this may be used in order to modulate effectively the intensity of photocurrents and emission of light from optoelectronic devices based on QR structures. The analogous effect relating to quantum wells was reported by Mendez *et al.*[8] Since the problem of the impurity electron in the QR in the presence of a strong electric field is not addressed in detail in the literature, we investigate this problem here. In the case where the electric field is parallel to the symmetry axis of the QR the ring topology is preserved but there is no significant effect on the radial states of the QR. For a strong in-plane electric field the ring topology is broken, leading to the disappearance of the unique ring properties. It is therefore most advantageous to apply a radially directed electric field created by a wire whose position coincides with the symmetry axis of the QR. In this case the electric field is directed radially and a strong influence on the radial motion is foreseen and, equally important, the topology of the QR is preserved.

In the present investigation of an impurity center in a semiconductor quantum ring in the presence of a radially directed electric field a twofold approach is pursued. First we will perform studies to obtain analytical (approximate) solu-

tions of the stationary Schrödinger equation in certain parameter regimes. This elucidates in particular the behavior and properties of the impurity binding for these regimes. Second, we perform a complementary numerical investigation that covers all possible cases (position of impurity, strength of the electric field, radii and height of the QR). Finally, exemplarily, a comparison of analytical and computational results is provided.

In detail we proceed as follows. Section II contains a general description of the setup—i.e., the quantum ring, the impurity, and the electric field configuration. Section III is devoted to the analytical investigation providing the method, the results, and their discussion. Section IV begins with an outline of our computational method followed by a comprehensive discussion of our numerical results. Section V provides a (naturally limited) comparison of the analytical and numerical results. Section VI contains the conclusions.

II. QUANTUM RING, IMPURITY, AND FIELD CONFIGURATION

We consider a QR formed by the revolution of a rectangle around the z axis. The plane of the rectangle contains the z axis. The QR is bounded by potential barriers of infinite height at the planes $z=\pm d/2$ and impenetrable cylindrical surfaces at internal $\rho=a$ and external $\rho=b$ radii. The chosen model corresponds to a hard-wall confinement potential. Alternatively, Chakraborty and Pietiläinen[9] proposed a parabolic ring confinement potential determined by the radius of the ring $\bar{\rho}$ and by the effective frequency Ω. This potential has been very effectively used in studies of QR's.[10–13] A comparison of the above-mentioned potential models is provided in Ref. 11.

The position of the impurity center $\boldsymbol{r}_0$ is determined by the cylindrical coordinates $a\leqslant\rho_0\leqslant b, \varphi_0=0$, and $-d/2\leqslant z_0\leqslant +d/2$. Additionally a radially directed electric field is provided by the field of a charged wire with linear effective charge density λ whose position coincides with the z axis. Furthermore, we take the conduction band to be parabolic, non degenerate, and separated from the valence band by a wide energy gap.

In the effective mass approximation the equation describing the impurity electron possessing the effective mass μ at a position $\boldsymbol{r}(\rho,\varphi,z)$ subject to the axially symmetric and radially directed electric field has the form

$$\left\{-\frac{\hbar^2}{2\mu}\left(\frac{1}{\rho}\frac{\partial}{\partial\rho}\rho\frac{\partial}{\partial\rho}+\frac{1}{\rho^2}\frac{\partial^2}{\partial\varphi^2}+\frac{\partial^2}{\partial z^2}\right)+\frac{e\lambda}{2\pi\varepsilon_0\varepsilon}\ln\frac{\rho}{a}-\frac{e^2}{4\pi\varepsilon_0\varepsilon[\rho^2-2\rho\rho_0\cos\varphi+\rho_0^2+(z-z_0)^2]^{1/2}}\right\}\Psi(\rho,\varphi,z)=E\,\Psi(\rho,\varphi,z), \tag{1}$$

where ε is the dielectric constant.

By solving this equation subject to the boundary conditions

$$\Psi(\rho,\varphi,z)=0 \text{ for } \rho=a,\quad \rho=b,\quad z=\pm d/2, \tag{2}$$

the total energy E and the wave function Ψ can be found in principle.

III. ANALYTICAL METHOD AND RESULTS

A. Adiabatic approach

We assume that the effects of the lateral (within the $x-y$ plane) confinement and of the electric field on the (bound) electron are taken to be much stronger than the influence of the Coulomb field of the impurity center. Under this condition the motion of the electron parallel to the z axis is adiabatically slower than the motion in the $x-y$ plane and the cylindrical variables ρ, φ, and z can be adiabatically separated. In the adiabatic approximation the wave function Ψ can be written in the form

$$\Psi(\rho,\varphi,z)=\Theta_{N,m}(\rho,\varphi)f^{N,m}(z), \tag{3}$$

where the function

$$\Theta_{N,m}(\rho,\varphi)=\frac{\exp(im\varphi)}{\sqrt{2\pi}}R_{N,m}(\rho) \tag{4}$$

describes the lateral motion of the electron of energy $E_{\perp N,m}$ determined by the radial confinement and the electric field. $R_{N,m}(\rho)$ is the Nth radial state function ($N=1, 2,\ldots$) possessing angular quantum number $m=0,\pm1,\pm2,\ldots$. It vanishes at $\rho=a$ and $\rho=b$ [see Eq. (2)]. The function $f^{N,m}(z)$ describes the longitudinal motion parallel to the z axis and satisfies the equation

$$-\frac{\hbar^2}{2\mu}\frac{d^2}{dz^2}f^{(N,m)}(z)+V_{N,m}(z)f^{(N,m)}(z)=W^{(N,m)}f^{(N,m)}(z), \tag{5}$$

with the boundary conditions

$$f^{(N,m)}(\pm d/2)=0 \tag{6}$$

and with the adiabatic potential

$$V_{N,m}(z)=-\frac{e^2}{4\pi\varepsilon_0\varepsilon}\int\frac{d\rho}{2\pi}\frac{|R_{N,m}(\rho)|^2}{[\rho^2-2\rho\rho_0\cos\varphi+\rho_0^2+(z-z_0)^2]^{1/2}}. \tag{7}$$

The binding energy $E_b=E^{(0)}-E$ of the impurity is defined as usual by the difference between the energy of the free electron in the QR, $E^{(0)}=E_{\perp N,m}+\hbar^2\pi^2l^2/2\,\mu\,d^2$, $l=1, 2,\ldots$, and the energy of the impurity electron, $E=E_{\perp N,m}+W^{(N,m)}$, which yields

$$E_b=\frac{\hbar^2\pi^2l^2}{2\,\mu\,d^2}-W^{(N,m)},\quad l=1,2,\ldots, \tag{8}$$

where the energy of the longitudinal state $W^{(N,m)}$ is obtained by solving Eq. (5).

B. Quasiclassical lateral states of the confined electron in the presence of an electric field

Let us first consider only the electron in the quantum ring; i.e., we omit the Coulomb term and the kinetic energy in the z direction in Eq. (1). Substituting

$$R_{N,m}(\rho)=\rho^{-1/2}\exp(x/2)u_{N,m}(x), \tag{9}$$

where

$$\rho = \rho_2 \exp x, \quad \rho_2 = a\exp(-x_1), \quad x_1 = -\frac{k^2}{s},$$

$$k^2 = \frac{2\mu E_{\perp N,m}}{\hbar^2}, \quad s = \frac{2\mu e\lambda}{\hbar^2 2\pi\varepsilon_0\varepsilon}, \tag{10}$$

we obtain the equation for the function $u_{N,m}(x)$:

$$u''_{N,m}(x) - [m^2 + s\rho_2^2 x\exp(2x)]u_{N,m}(x) = 0. \tag{11}$$

The boundary conditions (2) become $u(x_1)=u(x_2)=0$ and $x_2=\ln(b/a)+x_1$. Further we consider the cylindrically symmetric radial state only and the corresponding $m=0$ label will be dropped in the following.

Since Eq. (11) does not allow for an exact analytical solution for arbitrary magnitudes of the electric field, $\propto s$, a quasiclassical approach will be used. This method was developed originally for a free electron in an unbound medium in the presence of a radial electric field in Ref. 14. In case of a positively charged wire ($s>0$) attracting the electron to the internal surface of the QR the wave function $u_N(x)$ is given by the equation

$$u_N(x) = \left(\frac{4s}{\pi}\right)^{1/4} Q^{-1/2}(x)\cos\left[F(x) - \frac{\pi}{4}\right], \tag{12}$$

where $Q(x)=\rho_2 s^{1/2}(-x)^{1/2}\exp(x)$ and where

$$F(x) = \int_{x_1}^{x} Q(t)dt. \tag{13}$$

The parameters k and ρ_2 are determined by the Bohr-Sommerfield quantization rule

$$\int_{x_1}^{0} Q(t)dt = \pi(N+1/2), \quad N = 0,1,2,\ldots . \tag{14}$$

The limits of the integration in Eq. (14) $x=x_1$ and $x=0$ correspond to the near and far turning points $\rho=a$ and $\rho=\rho_2$. Note that the distance ρ_2 determines the region of the localization of the electron density. Under the condition $-x_1 \gg 1$ the integration in Eq. (14) can be performed explicitly, thereby providing the expressions for the energy of the lateral motion $E_{\perp N}$ (Ref. 14) and the radius of the Nth radial state ρ_{2N},

$$E_{\perp N} = \frac{\hbar^2 s}{2\mu}\ln\left(\frac{\rho_{2N}}{a}\right), \quad \rho_{2N} = \left(\frac{4\pi}{s}\right)^{1/2}(N+1/2), \tag{15}$$

as well as the function $F(x)$, Eq. (13), for $x_1 \leqslant x \leqslant 0$,

$$F(x) = \pi(N+1/2)\left(1 - \left[\Phi(\sqrt{-x}) - \frac{2}{\pi^{1/2}}\sqrt{-x}\exp x\right]\right), \tag{16}$$

where $\Phi(t)$ is the probability integral.[15] Equations (15) and (16) are valid under the conditions

$$\frac{a}{\rho_{2N}} \ll 1, \quad \ln\left(\frac{\rho_{2N}}{a}\right) \gg 1. \tag{17}$$

For the narrow QR satisfying the conditions

$$(b-a) \ll a,b, \quad \frac{(b-a)^3 s}{2\pi^2(N+1)^2 a} \ll 1,$$

the Bohr-Sommerfeld quantization rule

$$\int_{x_1}^{x_2} Q(t)dt = \pi(N+1), \quad N = 0,1,2,\ldots,$$

leads to the energy of the lateral motion:

$$E_{\perp N} = \frac{\hbar^2\pi^2(N+1)^2}{2\mu(b-a)^2} + \frac{e\lambda(b-a)}{4\pi\varepsilon_0\varepsilon\, a}. \tag{18}$$

This result coincides completely with that obtained in Ref. 3 where the Schrödinger equation was solved by means of perturbation theory. The energy $E_{\perp N}$, Eq. (18), is the size-quantized energy level in the two-dimensional (2D) quantum well of width $(b-a)$ perturbed by the homogeneous electric field with the effective strength $\lambda(4\pi\varepsilon_0\varepsilon\, a)^{-1}$.

For the negatively charged wire ($\lambda<0$) repulsion of the electron towards the external cylindrical surface of the QR leads to the Bohr-Sommerfeld rule

$$\int_0^{x_2} |Q(t)|dt = \pi(N+1/2), \quad N = 0,1,2,\ldots,$$

which yields for the lateral energy $E_{\perp N}$ the result

$$E_{\perp N} = -\frac{\hbar^2}{2\mu}|s|\ln\left(\frac{b}{a}\right) + \frac{\hbar^2}{2\mu}\left[\frac{3\pi(N+1/2)|s|}{2b}\right]^{2/3}. \tag{19}$$

This result is valid under the condition

$$\frac{2\pi^2(N+1/2)^2}{|s|b^2} \ll 1.$$

It follows from above that the energy $E_{\perp N}$, Eq. (19), is the sum of the lowest potential energy of the electron positioned at $\rho=b$ in the presence of the radial electric field and a perturbatively acting QR confinement.

Next we consider the positively charged wire ($\lambda>0$) and relatively wide QR for which the lateral energy $E_{\perp N}$ is given by Eq. (15). In parallel with this we assume that the condition

$$\rho_{2N} \ll a_0, \tag{20}$$

where $a_0=4\pi\varepsilon_0\varepsilon\,\hbar^2\mu^{-1}e^{-2}$ is the Bohr impurity radius, holds. This means that the effect of the electric field on the electron considerably exceeds the influence of the impurity center, so that the energy of the lateral motion $E_{\perp N}$ of the impurity electron is determined by the right-hand side of Eq. (15).

C. Binding energy of the impurity electron

1. 2D impurity states

Under the condition

$$d \ll a_0, \tag{21}$$

the states of the impurity electron have 2D character. In this case the total energy E can be written in the form

$$E = E_{\perp N} + \Delta E_N, \tag{22}$$

where $E_{\perp N}$ is given by Eq. (15) and where ΔE_N is determined by the matrix element of the Coulomb term on the left-hand side of Eq. (1) in which we neglect the dependence on the coordinate z. The matrix element is calculated with respect to the functions (9), (12), and (16) with the result

$$\Delta E_N = -4E_{\mathrm{Ry}}\left(\frac{a_0}{\rho_{2N}}\right)\left[\frac{1}{\pi}\ln\left(\frac{\rho_{2N}}{a}\right)\right]^{1/2}\left[1-\frac{\ln(\rho_0/a)}{2\ln(\rho_{2N}/a)}\right], \tag{23}$$

where $E_{\mathrm{Ry}}=\hbar^2/2\mu a_0^2$ is the impurity Rydberg constant. Equation (23) is valid under the conditions (17), (20), and (21) and $a \ll \rho_0 \ll \rho_{2N}$. The energy E, Eq. (22), is obtained by shifting the energy of the lateral motion of the free electron in the QR $E_{\perp N}$, Eq. (15), by the amount ΔE_N, Eq. (23), towards lower values of the energy. The binding energy $E_b = E_{\perp N} - E$ where E is given by Eq. (22) becomes $E_b = -\Delta E_N$ where ΔE_N is defined by Eq. (23).

2. 3D impurity states

For the relatively high QR satisfying the conditions

$$\rho_{2N} \ll d, a_0, \tag{24}$$

the motion of the electron parallel to the z axis described by Eq. (5) should be taken into account. The analysis of Eqs. (5)–(7) is based upon the Hasegawa-Howard method developed originally in Ref. 16 and was worked out in further detail in Ref. 17. The details of the application of this method to the problem of the impurity in the QR without field and in the presence of a strong magnetic field can be found in Ref. 3. It allows us to restrict ourselves to the transcendental equation for the quantum number determining the energy of the ground state of the longitudinal motion W.

(a) *High QR* ($d > a_0$). The equation for the quantum number $n<1$ determining the energy $W=-E_{\mathrm{Ry}}/n^2$ has the form

$$2C + \psi(1-n) + \frac{1}{2n} + \ln\left(\frac{\rho_{2N}}{a_0 n}\right) - \Delta(\rho_0) - \frac{1}{2}[G_1(z_0)+G_2(z_0)] = 0, \tag{25}$$

where C is the Euler constant ($\simeq 0.577$) and where $\psi(x)$ is the psi-function, the logarithmic derivative of the gamma function $\Gamma(x)$. The dependences of the energy W on the radial and longitudinal positions of the impurity center are given by the functions

$$\Delta(\rho_0) = \begin{cases} \Phi(y_0^{1/2})(1/2 - y_0) + y_0 - (y_0/\pi)^{1/2}\exp(-y_0) & \text{at } \rho_0 \leqslant \rho_{2N}, \\ y_0 & \text{at } \rho_0 \geqslant \rho_{2N}, \end{cases} \tag{26}$$

where $y_0 = -\ln(\rho_0/\rho_{2N})$ and

$$G_{1,2} = \Gamma(-n)\left(\frac{d}{a_0 n}\right)^{2n}\left\{\exp\left[\frac{d}{a_0 n}\left(1 \mp \frac{2z_0}{d}\right)\right] - 1\right\}^{-1}, \tag{27}$$

respectively. Equation (27) is valid under the condition

$$\left(\frac{d}{a_0 n}\right)^{2n} 4\sinh\left(\frac{2z_0}{a_0 n}\right)\left[\exp\left(\frac{d}{a_0 n}\right) - 2\cosh\left(\frac{2z_0}{a_0 n}\right)\right]^{-1} \ll 1. \tag{28}$$

Note that Eq. (28) does not significantly limit the displacement of the impurity z_0 from the symmetric plane of the QR ($z=0$). For the QR of height $d \simeq 2a_0$ subject to the radial electric field providing the relationship $\rho_{2N} \simeq 0.4a_0$ and for the impurity being positioned close to the midplane ($z_0=0$) and the internal surface ($\rho_0 \simeq a, y_0 \gg 1$), Eq. (25) yields for the quantum number $n \simeq 0.5$. Even though the impurity is shifted by a considerable distance $z_0 = d/4$ the term on the left-hand side of Eq. (28) is about 0.3. In principle Eq. (25) can be solved numerically for arbitrary values of the height of the QR $d > a_0$ and the impurity position $\rho_0, d/2 - |z_0| \gg \rho_{2N}$. However, the explicit dependences of the energy W on the above-mentioned parameters can be found for the limiting cases of small displacements z_0 from the symmetric plane of the QR ($2z_0/d \ll 1$), for $a \ll \rho_0 \ll \rho_{2N}$ and a maximum ($\rho_0 \simeq b \gg \rho_{2N}$) shift ρ_0 of the impurity from the symmetric axis $\rho=0$.

For small displacements $2z_0/a_0 n \ll 1$ the dependence of the quantum number $n(z_0)<1$ and the energy W of the ground state as a function of the displacement z_0 can be found explicitly from Eq. (25) with the result

$$W(z_0,\rho_0) = -\frac{E_{\mathrm{Ry}}}{n_1^2}\left[1 - 2\Gamma(1-n_1)\left(\frac{2z_0}{a_0 n_1}\right)^2\left(\frac{d}{a_0 n_1}\right)^{2n_1} \times \exp\left(-\frac{d}{a_0 n_1}\right)\right], \tag{29}$$

where n_1 is the solution to Eq. (25) for $z_0=0$ and for any radii ρ_0.

The effect of the radial displacement ρ_0 is described by the function $\Delta(\rho_0)$, Eq. (26). For $\rho=\rho_{2N}$ we have $\Delta=0$ and with decreasing (increasing) ρ_0 the function $\Delta(\rho_0)$ increases (decreases) towards the internal (external) boundary of the QR. We obtain, from Eq. (26),

$$\Delta(\rho_0) = \begin{cases} \frac{1}{2} & \text{for } (\rho_0 - a) \ll a, \\ \frac{\rho_{2N}-\rho_0}{\rho_{2N}} & \text{for } |\rho_0 - \rho_{2N}| \ll \rho_{2N}. \end{cases} \tag{30}$$

For small radial displacements from $\rho_0=\rho_{2N}$ for which $4n\Delta \ll 1$ [see below Eq. (30)], Eq. (25) gives the approximate expression for the quantum number n and then for the energy of the ground state W:

$$W(z_0,\Delta) = -\frac{E_{\mathrm{Ry}}}{n_2^2}\left[1+\frac{4n_2}{1+2n_2}\Delta(\rho_0)\right], \tag{31}$$

where n_2 is the solution to Eq. (25) for $\Delta(\rho_{2N})=0$ and any positions z_0.

In the logarithmic approximation $[\rho_{2N}/a_0 \ll 1, |\ln(\rho_{2N}/a_0)| \gg 1]$ the quantum number n can be calculated from Eq. (25) explicitly:

$$\frac{1}{n} = 2\left\{-\ln\left(\frac{\rho_{2N}}{a_0}\right)+\Delta(\rho_0)+\frac{1}{2}[G_1(z_0)+G_2(z_0)]\right\}. \tag{32}$$

It follows from Eq. (8) that the binding energy E_b of the impurity electron in the high QR can be written in the form

$$E_b = E_{\mathrm{Ry}}\left[\left(\frac{\pi a_0}{d}\right)^2+\frac{1}{n^2}\right], \tag{33}$$

where the quantum number n can be found from Eq. (25) to give particularly in the above-mentioned logarithmic approximation the expression (32). It enables us to investigate qualitatively the dependence of the binding energy E_b on the internal radius a and height d of the QR, the strength of the electric field s, and the position of the impurity center z_0, ρ_0. We emphasize that the logarithmic approximation is used only for a qualitative analysis.

(b) *Low QR* $(d<a_0)$. For positive energies $W=E_{\mathrm{Ry}}/s^2$ in Eq. (5) using the procedure presented in detail in Ref. 3 we obtain the transcendental equation for the quantum number s:

$$\tilde{\varphi}(s)+\ln\left(\frac{\rho_{2N}}{a_0 s}\right)-\Delta(y_0)+1-\frac{1}{2}\left[\tilde{G}_1(z_0)+\tilde{G}_2(z_0)\right]=0. \tag{34}$$

In Eq. (34) the following notations are employed:

$$\tilde{\varphi}(s) = \frac{\tilde{\Gamma}(s)}{2i}\left\{\frac{1}{\Gamma(is)}\left[\frac{i\pi}{2}+2C-1+\psi(1+is)-\frac{1}{2is}\right]-\mathrm{c.c.}\right\},$$

$$\frac{1}{\tilde{\Gamma}(s)} = \frac{1}{2i}\left[\frac{1}{\Gamma(is)}-\frac{1}{\Gamma(-is)}\right],$$

$$\tilde{G}_{1,2}(z_0) = \tilde{\Gamma}(s)\frac{\mathrm{Re}\, W_{is,1/2}(\tau_{1,2})}{\mathrm{Im}\, M_{is,1/2}(\tau_{1,2})}, \quad \tau_{1,2} = \frac{2}{ia_0 s}\left(\frac{d}{2}\mp z_0\right).$$

Equation (34) can be solved explicitly for $s \ll 1$ to give for the energy of the ground state W:

$$W = \frac{\hbar^2\pi^2}{2\mu d^2}+\Delta W, \tag{35}$$

where

$$\Delta W = -2E_{\mathrm{Ry}}\left(\frac{a_0}{d}\right)\left\{-4\left[C-\Delta(\rho_0)+\ln\left(\frac{\pi\rho_{2N}}{d}\right)\right]\cos^2\left(\frac{\pi z_0}{d}\right)+\ln\left[\pi^2\left(1-\frac{4z_0^2}{d^2}\right)\right]\right\}. \tag{36}$$

Equations (35) and (36) are valid under the conditions (24) and $d \ll \pi a_0$. The energy W, Eq. (35), is the size-quantized ground energy level of the electron in the quantum well of width d shifted towards lower energies by an amount of ΔW, Eq. (36), associated with the impurity field. Substituting the energy W, Eq. (35), into the right-hand side of Eq. (8) taken for $l=1$ we obtain for the binding energy E_b of the impurity electron in the low QR the result $E_b=-\Delta W$, where ΔW is given by Eq. (36).

D. Discussion of the analytical results

1. 2D impurity states

The binding energy E_b of the 2D states has the form $E_b=-\Delta E_N$ where the correction to the lateral energy caused by the impurity attraction is given by Eq. (23). It is clear from Eq. (23) that the binding energy decreases with an increase of the internal radius of the QR, a. Also the binding energy decreases with increasing the radial displacement ρ_0 of the impurity center from the internal surface of the QR in the region $a \ll \rho_0 \ll \rho_{2N}$. Since the strong electric field concentrates the electron density close to the internal surface $\rho \simeq a$, the greater the distance ρ_0-a between this surface and the impurity center is, the less the impurity attraction—i.e. the less the binding energy. For the impurity positioned in the region $a \ll \rho_0 \ll \rho_{2N}$ the binding energy increases with increasing electric field strength $\propto s$. The increasing electric field shifts the electron density distributed between $\rho \simeq a$ and $\rho \simeq \rho_{2N}$ towards the impurity center positioned at $\rho_0 \ll \rho_{2N}$. This leads to an increase in binding energy.

2. 3D impurity states, high QR

The binding energy E_b of the 3D states in the high QR $(d>a_0)$ is provided by Eq. (33). The corresponding quantum number n can be found in principle from Eq. (25). In the logarithmic approximation the quantum number n is determined by Eq. (32). Since the contribution of the second term on the right-hand side of Eq. (33) is exponentially small compared to the size-quantized energy $(\sim 1/d^2)$ [see Eq. (29)], the binding energy decreases with an increase of the height of the QR, $d>a_0$. Clearly from Eqs. (32) and (33) we see that the binding energy increases with increasing the electric field. The greater the electric field is, the less the effective radius of the lateral motion $\rho_{\mathrm{eff}} \sim \rho_{2N}$ and the greater the depth of the one-dimensional potential $V_{N,0}$, Eq. (7), governing the longitudinal motion between the bottom and top of the QR. This leads to an increase with respect to the binding energy E_b. Expressions (8) and (29) show that the impurity being positioned at the midplane $z=0$ produces the greatest binding energy. The shift of the impurity center z_0 from the midplane $z=0$ causes a decrease of the binding energy E_b. Narrowing the QR or increasing the electric field

strength increases the energy shift $\Delta E_b(z_0)$ associated with the displacement of the impurity from the plane $z_0=0$ in both cases.

The radial shift of the impurity center ρ_0 from the some intermediate position ρ_{0m} towards the internal $\rho=a$ and external $\rho=b$ surfaces produces similar effects as those induced by the displacement z_0 from the midplane $z=0$. It follows from Eqs. (26), (30), (32), and (33) that for QR's possessing an external radius b comparable to the impurity Bohr radius a_0 the binding energy $E_b(\rho_0)$ at $\rho_0=a$ approximates that of $\rho_0=b$ both being determined by the quantum number $n \simeq [-2\ln(\rho_{2N}/a_0)]^{-1}$. Since the parameter $\Delta(\rho_0)$, Eq. (30), and quantum number n^{-1}, Eq. (32), both increase with the displacement of the position ρ_0 from the external surface $\rho_0=b$ towards the internal one $\rho_0=a$, we expect that the binding energy $E_b(\rho_0)$ reaches a maximum at a certain radial position ρ_{0m}. The shift of the binding energy induced by a radial displacement ρ_0 possesses a maximum for the impurity positioned at the plane $z_0=0$ and decreases with increasing displacement from this plane.

It follows from the above that the corrections to the binding energy induced by the displacements from, say, the circle $\rho_0 \simeq \rho_{2N}, z_0=0$ to the region $a \leqslant \rho_0 < \rho_{2N}, |z_0|>0$ can cancel each other.

3. 3D impurity states, low QR

It is clear that the binding energy $E_b=-\Delta W$, Eq. (36), increases with a decrease of the height $d<a_0$ of the QR and with increasing strength of the electric field strength. For small displacements $2z_0/d \ll 1$ from the midplane $z_0=0$ we obtain, from Eq. (36),

$$E_b(z_0) = E_{b1}(0) + 2E_{\mathrm{Ry}}\left(\frac{a_0}{d}\right)\left(\frac{2z_0}{d}\right)^2\left\{-1+\pi^2\left[C-\Delta(\rho_0)+\ln\left(\frac{\pi\rho_{2N}}{d}\right)\right]\right\}, \tag{37}$$

where

$$E_{b1}(0) = -8E_{\mathrm{Ry}}\left(\frac{a_0}{d}\right)\left[C-\Delta(\rho_0)+\ln\left(\frac{\pi^{1/2}\rho_{2N}}{d}\right)\right]$$

is the binding energy of the impurity positioned at the midplane $z_0=0$ and any radial distances ρ_0. The shift of the impurity from the point z_0 leads to a decrease with respect to the binding energy. With increasing electric field strength we observe an increase of the shift of the binding energy caused by the displacement z_0.

The dependence of the binding energy on the radial position ρ_0 can be derived from Eq. (36):

$$E_b(\Delta) = E_{b2}(0) + 8E_{\mathrm{Ry}}\left(\frac{a_0}{d}\right)\Delta(\rho_0)\cos^2\left(\frac{\pi z_0}{d}\right), \tag{38}$$

where

$$E_{b2}(0) = 2E_{\mathrm{Ry}}\left(\frac{a_0}{d}\right)\left\{-4\left[C+\ln\left(\frac{\pi\rho_{2N}}{d}\right)\right]\cos^2\left(\frac{\pi z_0}{d}\right)+\ln\pi^2\left(1-\frac{4z_0^2}{d^2}\right)\right\}$$

is the binding energy of the impurity positioned at the point $\rho_0=\rho_{2N}$ for which $\Delta(\rho_{2N})=0$ and at any plane z_0. The binding energy E_b, Eq. (38), decreases if the impurity center moves from the certain position ρ_{0m} towards the radial boundaries of the QR. The shift of the binding energy associated with the parameter $\Delta(\rho_0)$ reaches a maximum for the impurity center positioned at the plane $z_0=0$ and decreases with increasing displacement from this plane. For a low QR the corrections to the binding energy induced by the radial (ρ_0) and vertical (z_0) displacements can be chosen such that they cancel each other; i.e., in this case there is no resulting change of the energy for specific shifts from the circle $\rho_0 \simeq \rho_{2N}, z_0=0$ to the region $a \leqslant \rho_0 < \rho_{2N}, |z_0|>0$. Thus the dependences of the impurity binding energy E_b on the strength of the electric field, the height of the QR, d, and the position of the impurity within the QR, ρ_0, z_0, are qualitatively the same both for high and low QR's.

IV. NUMERICAL APPROACH

A. Computational method

Our numerical approach to solve Eq. (1) is a finite-difference method, described in detail in Refs. 18–20 for two-dimensional systems and in Refs. 21 and 22 for three-dimensional systems. We have solved Eq. (1) in cylindrical coordinates (ρ, ϕ, z) in a region Ω,

$$a \leqslant \rho \leqslant b,$$

$$0 \leqslant \phi \leqslant \pi,$$

$$-d/2 \leqslant z \leqslant d/2, \tag{39}$$

respecting the boundary conditions (2)—i.e., with $\Psi=0$ on the boundaries in coordinates ρ and z and with condition $\partial\Psi/\partial\phi|_{\phi=0,\pi}=0$ for ϕ. Our computational procedure consists of the following main steps. The nodes of the spatial mesh are chosen in the domain Ω, and the values of the wave function at the nodes represent solutions of the initial differential equation (1). Since the domain Ω is bounded with respect to all three coordinates, we can use uniform meshes. The nodes of these meshes have coordinates $\rho_i=a+(b-a)(i-1/2)/N_\rho$, $\phi_j=\pi(j-1/2)/N_\phi$, and $z_k=-d/2+d(k-1/2)/N_z$, $i=1,\ldots,N_\rho$, $j=1,\ldots,N_\phi$, and $k=1,\ldots,N_z$. After replacing the derivatives by their finite-difference approximations Eq. (1) takes the form of a system of linear equations for Ψ values at the nodes and approximate values of energy can be found as eigenvalues of the corresponding Hermitian matrix. The final values for the energy are provided by using the Richardson extrapolation technique for the corresponding results emerging from a series of geometrically similar meshes with different number of nodes—i.e., eigenvalues obtained for meshes with $N_\rho=KN_{\rho 0}, N_\phi$

$=KN_{\phi 0}$, and $N_z=KN_{z0}$, where $K=1, 2,\ldots$. Using this approach we achieve a major increase of the numerical precision and, in particular, we obtain together with each numerical value a reliable estimate of its precision. Typical numbers of mesh nodes used in the present calculations were of order 40^3—i.e., 40 nodes in each direction for the thickest (corresponding to maximal values of K) meshes. An important factor affecting the choice of values $KN_{\rho 0}, KN_{\phi 0}$, and KN_{z0} is the position of the Coulomb center, which does not coincide with the origin of the coordinate system. A geometrical similarity of meshes with different K can be achieved only when this center has coordinates $[a+(b-a)i/N_{\rho 0}, \pi j/N_{\phi 0}, -d/2 + dk/N_{z0}]$. This circumstance affects the choice of coordinates of the Coulomb center and sometimes required calculations on meshes containing more nodes than absolutely needed for obtaining a satisfactory numerical precision. Along with solutions of Eq. (1) in its general 3D form we have solved the corresponding equation in two dimensions employing the coordinates $(\rho, \phi)(z=z_0)$. This allows us to obtain the binding energy of the electron in the limit $d \to 0$. The numerical solution has no additional specific features compared to the 3D one.

B. Numerical results and discussion

We present here detailed results on the binding energy of the electron for two fixed geometries of the quantum ring, referred to in the following as (A) and (B) corresponding to realistic experimental parameters (see below). Some additional results on the dependences of this energy on the geometry of the quantum ring are also presented. Parameters of the quantum ring (A) are GaAs is the ring material, GaAlAs is the barrier material, $a=5$ nm, $b=20$ nm, and $d=15$ nm. For the quantum ring (B), $a=10$ nm, $b=40$ nm, and $d=3$ nm with InAs as the ring material and GaAs as the barrier material. In order to simplify the comparison of the results for rings made of different materials we transform the values of parameters into effective atomic units (e.a.u.). Using parameters $\epsilon=12.56$ and $\mu=0.067m_0$ for GaAs and $\epsilon=14.5$ and $\mu=0.023m_0$ for InAs we obtain $a=0.5, b=2$, and $d=1.5$ for ring (A) and $a=0.3, b=1.2$, and $d=0.09$ for (B). The case (A) means a ring with its height being comparable with the other dimensions, whereas case (B) is a low ring with $d \ll a, b$.

In the following we will particularly consider the binding energy E_b of the electron as a function of various parameters. The binding energy is the difference between the total energy of the electron obtained in our numerical calculations and the energy E_0 of the electron in the same quantum ring without the impurity center. The latter energy consists of two terms

$$E_0 = E_{\|0} + E_{\perp 0}, \tag{40}$$

where $E_{\|0}$ and $E_{\perp 0}$ are the energies of the motion in the z direction and of the lateral motion in the plane (ϕ, ρ), respectively. An exact analytical expression for the first of them is given in Eq. (8) and for the ground state looks for effective atomic units as $E_{\|0}=\pi^2/2d^2$. The second term does not depend on d and can be easily calculated numerically for each set of parameters (a, b, λ) by solving a two-dimensional version of Eq. (1) for very large values of ρ_0. In Fig. 1 we show $E_{\perp 0}(\lambda)$ for several geometries. They include $E_{\perp 0}(\lambda)$ for QR's (A) and (B) as well as two dependences for a small inner radius $a=0.125$ e.a.u. and different b. For large positive λ these functions are near to linear ones owing to the concentration of the electron density in a small vicinity of the inner boundary of the quantum ring. In result the curves for $a=0.125$ e.a.u. and different b coincide for this range of λ. The slope of the curves for positive λ is determined by a and increases with a decrease of this value. For large negative λ the functions $E_{\perp 0}(\lambda)$ also have a linear form with slopes depending on both a and b.

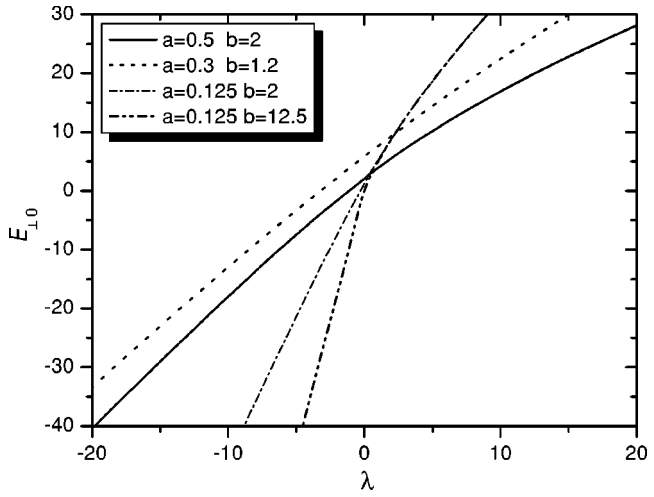

FIG. 1. Energy of the lateral motion a free electron in a quantum ring as a function of the charge λ of the central wire. Effective atomic units are used.

In Fig. 2 we present E_b as a function of the position (z_0, ρ_0) of the impurity center for quantum ring (A). The binding energy shows a significant dependence on ρ_0 and λ for $z_0 \ll d/2$ whereas for z_0 being close to $\pm d/2$ the dependence on ρ_0 is much less pronounced. The dependence of E_b on ρ_0 and λ for $z_0=0$ is presented in Fig. 3. It should be noted that the effect of the radial electric field on the binding energy is much less compared to its effect on the total energy. For example, the maximal value of the difference $E_b(\lambda=10)-E_b(\lambda=0)$ (for $\rho_0=0.875$) is 0.495 e.a.u., whereas

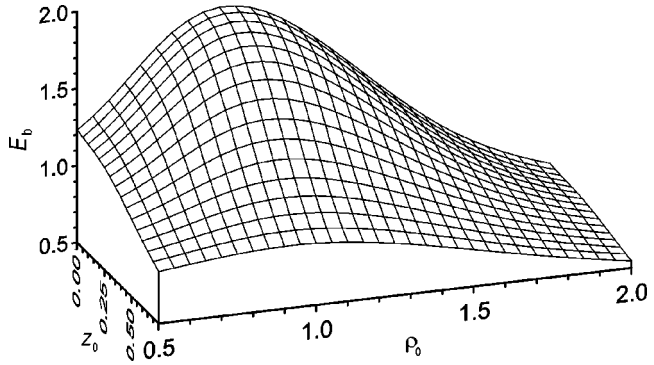

FIG. 2. Binding energy E_b as a function of the position of the impurity center for quantum ring (A) $\lambda=4.3$ of the central wire. Effective atomic units are used.

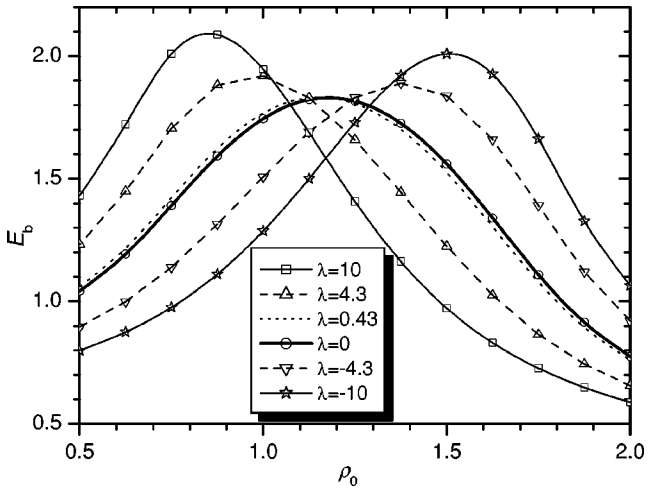

FIG. 3. Binding energy E_b as a function of the radial position of the impurity center ρ_0 for quantum ring (A) for $z_0=0$ for several different values of the linear charge density λ of the central wire. Effective atomic units are used.

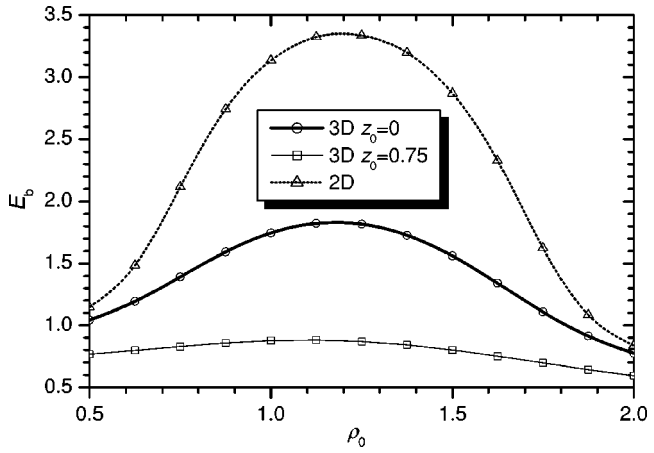

FIG. 4. Binding energy E_b as a function of the radial position of the impurity center ρ_0 for quantum ring (A) for $\lambda=0$ and for different displacements $z_0=0, z_0=d/2$ and the corresponding 2D quantum ring ($d=0$). Effective atomic units are used.

the corresponding difference for E_0 (or $E_{\perp 0}$) is 14.81 e.a.u. However, the relative change of E_b due to the external field is of the order of 100%.

For $\lambda=0$ the binding energy presented in Fig. 2 achieves its maximum (at ρ_{0m}) close to the middle point of the radial cross section of the quantum ring. This is due to the fact that the energy of the ground state of a hydrogenlike system increases when the system approach a impenetrable potential wall. In the case of a flat infinite wall the ground state of a hydrogen atom with the nucleus lying on the boundary of the wall is similar to the state $2p_0$ of the free hydrogen atom and has energy −0.125 a.u. instead of −0.5 a.u. for the ground state of the free atom. Since E_0 does not depend on the position of the impurity center, approaching the boundaries of the quantum ring equally affects the value of the total energy and the value of the binding energy E_b. On the other hand, positive values of E_0 for spatially confined systems ($\lambda=0$) increase the binding energy compared to a free impurity center. As a result the impurity electron in the quantum ring is more tightly bound for all the parameter values presented in Fig. 3 compared to the case of an impurity center in a bulk. However, the total energies of the electron are higher compared to the case of a bulk.

The asymmetry of the curve for $\lambda=0$ and in particular a higher binding energy at $\rho_0=a$ compared to $\rho_0=b$ are due to the curvature of the boundaries of the quantum ring. In the case of the inner $\rho_0=a$ boundary its curvature provides more space for the motion of the electron compared to a corresponding flat wall. As a result the motion of the electron is less confined and its energy is lower than for the case of a flat wall and is closer to the values for the case where the center is far from the boundaries. The opposite curvature of the outer $\rho_0=b$ boundary of the quantum ring leads to the opposite effect consisting of a decrease of the binding energy for the impurity center near to this boundary.

For both positive and negative λ the maxima of the energy curves $E_b(\rho_0)$ exceed that corresponding to $\lambda=0$. This effect is fully analogous to the quadratic Stark effect, which leads to a decrease of the ground-state energy level and to an increase of the binding energy of the hydrogenlike impurity electron in the presence of external electric field. The shifts of the positions of the maximums to the left-hand side for $\lambda>0$ and to the right-hand side for $\lambda<0$ are explained by the increase of the binding energy for smaller distances ρ_0 in the case of an attractive positively charged wire or for larger distances in the case of a negatively charged wire.

Figure 3 (curves corresponding to $\lambda=\pm 4.3$) demonstrates that in the impurity QR the inversion effect of the electric field occurs. The binding energy $E_b(\lambda)$ changes as the direction of the electric field λ changes ($+\lambda \rightarrow -\lambda$). An analogous effect relating to a quantum well structure was studied in Ref. 23. In contrast to the quantum well in which the inversion shift of the binding energy $\Delta E_b=E_b(+\lambda)-E_b(-\lambda)$ vanishes for the impurity center positioned at the midplane ($z_0=0$), the inversion shift in the QR is absent for a certain ($\rho_0=1.15$) cylindrical surface.

In Fig. 4 we compare the binding energies $E_b(\rho_0)$ for quantum ring (A) for $z_0=0, z_0=d/2$ and for a 2D quantum ring with the same values of a and b. We observe a much weaker dependence of the binding energy for $z_0=d/2$ on the radial position of the impurity center compared to the case $z_0=0$. On the other hand, the curve for $z_0=0$ is much lower in energy and demonstrates a weaker dependence on ρ_0 compared to the 2D curve. The large difference between 2D and 3D binding energies is due to the large value of d for quantum ring (A) and strong confinement provided by the 2D QR. The predominant part of the curve E_b for the two-dimensional impurity is above $E_b=2$. The latter is the binding energy for a two-dimensional impurity without external confinement for the motion in ρ direction—i.e., a bulk impurity. The above-mentioned difference reflects the increase of the binding energy due to the confinement in the radial ρ direction.

The opposite case of a low quantum ring is shown in Fig. 5 where the corresponding energy curves analogous to those of Fig. 4 are presented for quantum ring (B). For $\lambda=0$ the behavior is qualitatively very similar to the one observed in

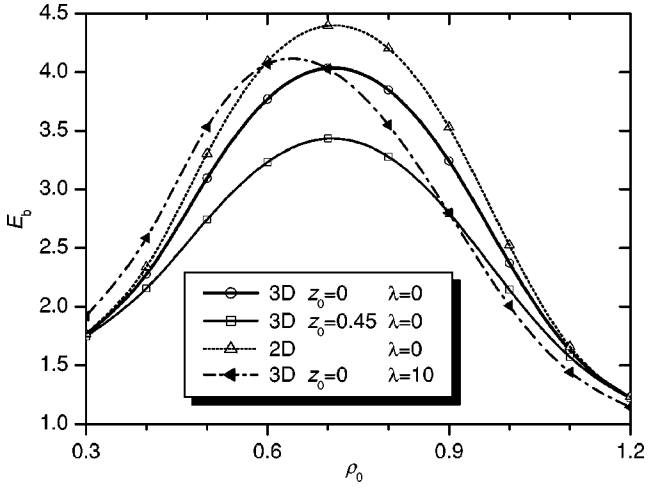

FIG. 5. Quantum ring (B): same as Fig. 4 and a 3D curve for $\lambda=10, z_0=0$. Effective atomic units are used.

Fig. 4 with the exception that both 3D energy curves are much closer to the 2D curve than for quantum ring (A). Figure 5 contains also an energy curve for a nonzero radial electric field, corresponding to $\lambda=10$. One can see that the radial electric field has a minor effect for the low QR (B) compared to the high QR (A). This is due to the quantitatively reduced effect of an external electric field on 2D hydrogenlike systems compared to 3D ones (see Refs. 24 and 25 and references therein).

The presence of maxima for the energy functions $E_b(\rho_0)$ and the shifts of these maxima with changing radial electric field strength determine the form of these functions $E_b(\lambda)$ presented in Fig. 6. For the impurity being centered in the z direction ($z_0=0$) we present five curves for different positions ρ_0 in the radial direction. Let us discuss some major properties of these curves. It is straightforward to understand the behavior of the two curves for $\rho_0=1$ and $\rho_0=1.25$ corresponding to the impurity center positioned near to the middle of the QR in the radial direction. These curves have maxima in the vicinity of $\lambda=0$. This means that the presence of a

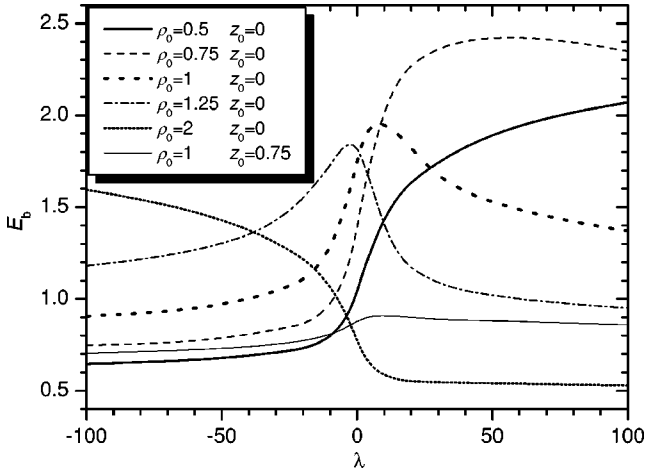

FIG. 6. Binding energy E_b as a function of the central wire charge λ for the different impurity positions ρ_0, z_0 in quantum ring (A). Effective atomic units are used.

strong radial electric field (independent of its direction) decreases the binding energy of the electron to the impurity center for these values of ρ_0. This decrease of the binding energy originates from a decrease of the electronic density near the impurity center, because the radial electric field either attracts the electronic density to the inner boundary of the ring or repels it towards the outer boundary. The curves $E_b(\lambda)$ for the two opposite cases when the impurity center is situated directly on the inner $\rho_0=0.5$ or on the outer $\rho_0=2$ boundary of the QR possess no maxima. They show an increase of the binding energy when the radial electric field attracts the electronic density to the impurity center and a decrease of E_b when it repels the electronic density to the opposite boundary. If the boundaries were flat and infinite in the z direction the limiting values of the binding energy both for $\rho_0=0.5$ and $\lambda\to+\infty$ and for $\rho_0=2$ and $\lambda\to-\infty$ would correspond to the ground state of a two-dimensional hydrogen atom $E_b=2$ (the mutual action of the electric field and the impenetrable potential wall would provide a confinement of the electron in the plane). In the QR the outer boundary provides less space for the motion of the electron in the corresponding limit in comparison with the inner boundary. As a result we may expect that the limiting value of E_b for $\rho_0=0.5, \lambda\to+\infty$ should be larger than E_b for $\rho_0=2, \lambda\to-\infty$. This is in agreement with the behavior of the corresponding curves in Fig. 6. For the two opposite limits $\rho_0=0.5, \lambda\to-\infty$ and $\rho_0=2, \lambda\to+\infty$ $E_b(\lambda)$ becomes asymptotically flat. This is due to the fact that when practically all the electronic density is concentrated at the opposite boundary its small redistribution in strong fields does not affect (due to different but large λ values) the interaction with the impurity center. The energy of this interaction depends on the average distance between the electron and impurity center. Due to the confinement of the electron on the inner or outer surface of the quantum ring, the latter problem acquires some similarity with the electrostatic problem of a charge near a conducting surface. The potential of the interaction of a charge with its image in a convex surface is smaller than the interaction of the charge with a mirror charge in a flat or a concave surface (compare with Ref. 26). These reasons explain the result $E_b(\rho_0=0.5, \lambda\to-\infty) > E_b(\rho_0=2, \lambda\to+\infty)$.

As an example of $E_b(\lambda)$ for an impurity center located at a small distance from one of the boundaries we show in Fig. 6 a curve for $\rho_0=0.75$ and $z_0=0$. In agreement with the picture presented above it has a maximum in a region of positive λ. The binding energy in the vicinity of this maximum is higher than that for maxima of the corresponding curves for $\rho_0=1$ and $\rho_0=1.25$ because the radial electric field can concentrate a larger electronic density at smaller ρ. Finally we present also $E_b(\lambda)$ for $\rho_0=1$ and $z_0=0.75$—i.e., for the impurity being located on the top boundary of the QR. The behavior of this curve is similar to curves for $z_0=0$, but both the absolute values of E_b and their alterations are smaller. Note that in the QR the radial electric field may cause the impurity electron to be more stable while in the bulk material the electric field leads to the ionization of the impurity center.

The obtained results allow us to estimate the values to be expected in an experiment. It follows from Fig. 6 that the

positive shift of the binding energy $\Delta E_b(\lambda)$ of the impurity positioned at $z_0=0$ and $\rho_0=7.5$ nm in the QR(A) caused by a positive electric field λ of a charged wire having the linear electron density $n_e=5\times10^6$ cm^{-1} amounts to $\Delta E_b \simeq 4.5$ meV. The relative change is therefore $\Delta E_b(\lambda)/E_b(0) = 0.28$. In this electric field a decrease of the binding energy $\Delta E_b \simeq -11.6$ meV (about 52%) occurs if we shift the impurity center from the symmetric plane $\rho_0=10$ nm, $z_0=0$ to the boundary plane $\rho_0=10$ nm, $z_0=7.5$ nm. When the impurity center moves in the symmetric plane ($z_0=0$) of the QR(A) (see Fig. 3) subject to the positive electric field $\lambda=4.3$ determined by the linear electron density $n_e=4.3\times10^6$ cm^{-1} from the internal boundary $\rho_0=5$ nm to the position $\rho_0=10$ nm the binding energy E_b increases by an amount $\Delta E_b \simeq 8.1$ meV. This is about 58% of the binding energy $E_b(\rho_0)$ at $\rho_0=a$. In this field the inversion shift of the binding energy $\Delta E_b(\lambda) = E_b(-\lambda)-E_b(+\lambda)$ for the case $z_0=0, \rho_0=15$ nm is $\Delta E_b \simeq 7.5$ meV. The inversion shift vanishes at $\rho_0=11.5$ nm. The estimates of the expected values for the InAs/GaAs QR can be made accordingly using the parameters of the InAs material, providing values of the same order of magnitude as those for the GaAs QR. Thus the obtained effects induced by the radial electric field in the impurity QR are detectable in an experiment.

Concerning the currently available experimental data to our knowledge most of them are related to the persistent current occurring in the QR threaded by the magnetic field (see Ref. 6 and references therein). The effect of an electric field is studied theoretically[4–6] for the case of a uniform electric field directed parallel to the plane of the QR. One of the reasons (concerning both theory and experiment) to choose this configuration is that the electric field has been treated as a tool acting on the electron states, causing in particular the breaking of the axially symmetric potential of the QR and mixing the states with different angular quantum numbers. No additional serious experimental refinements specifically associated with the QR's are required. However, the radially directed electric field considered in our paper is capable on the one hand of conserving the axial symmetry of the QR potential and on the other hand of modifying strongly the impurity states in the QR. Let us briefly address the question of the experimental realization of the additional electric field. A Si wire covered by the exact-position-monitored charge being embedded in the inner region of the QR offers a source of the radial electric field. Particularly these wires of about 10 nm diameter are employed in the silicon-based charge-coupled devices.[27] An alternative approach would be as follows. The inner region of the QR is doped by the shallow impurity centers. Being activated these centers become charged and this region can be treated as the source of the radial electric field for the QR. We believe that our results could stimulate experiments that contribute to the physics of QR's and their optical-electronic applications.

V. COMPARISON OF NUMERICAL AND ANALYTICAL RESULTS

We present in this section an exemplary comparison of our numerical and analytical results. Figure 7 shows numerically calculated energies for a free electron in three different two-dimensional quantum rings. These energies are given as functions of the logarithm of the positive charge density on the central wire. For a QR with small $a=0.125$ and very large $b=12.5$ the numerical curve for $E(\lambda)$ presented on a double-logarithmic scale is not very different from a straight line. The formula (15) provides a good approximation for this curve for not too large values of λ. The discrepancy at large λ is due to small values of $\rho_{2N}(\rho_{2N}<a)$ given by Eq. (15). A major improvement of the analytical estimation could be achieved by replacing the formula for ρ_{2N} by

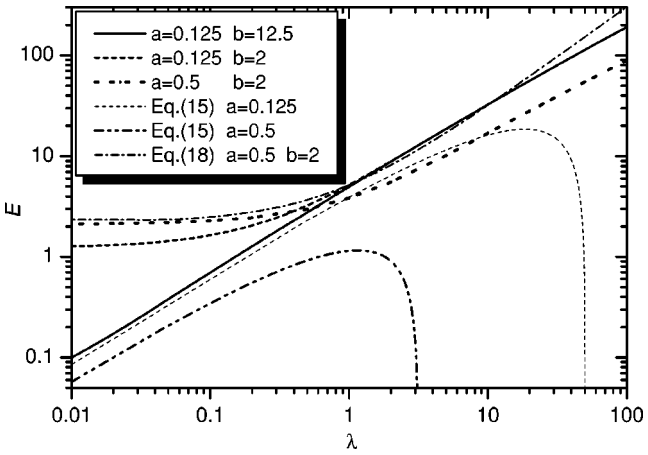

FIG. 7. Energy of a free electron in three different two-dimensional quantum rings as a function of the positive charge of the central wire λ. Numerical results and analytical estimations are shown. Effective atomic units are used.

$$\rho_{2N} = \left(\frac{4\pi}{s}\right)^{1/2}(N+1/2)+a. \tag{41}$$

The numerically calculated curve for $a=0.125$ and $b=2$ coincides with that for $a=0.125$ and $b=12.5$ for large values of λ. As $\lambda\to0$ the value of E converges to a finite limit, determined by the energy of an electron in a finite 2D quantum ring. This energy increases when the ring becomes narrower as can be seen when comparing the curves for $a=0.125$ and $b=2$ and for $a=0.5$ and $b=2$. For large λ the latter curve shows also approximately a linear behavior but is lower in energy than the curves for $a=0.125$. This shift is properly described by Eq. (15), but the relatively small value $b=2$ does not allow one to obtain estimations for the energy of the free electron for $a=0.5$ and $b=2$ by Eq. (15). For this set of parameters we present in Fig. 7 also the energy given by Eq. (18). One can see that even for such a broad QR this formula gives quite a reasonable approximation to the energy. For $(b-a)\ll a,b$ this formula is in very good agreement with the numerical data.

In Fig. 8 analytical estimates given by Eq. (23) for the binding energy of an electron in two-dimensional quantum rings in the presence of an impurity are compared with the corresponding numerical results. Equation (23) includes ρ_{2N} values given by Eq. (15) and this circumstance restricts the applicability of it for strong fields. Condition $\rho_{2N}\ll a_0$, or $\rho_{2N}\ll1$ in effective atomic units, restricts the applicability of

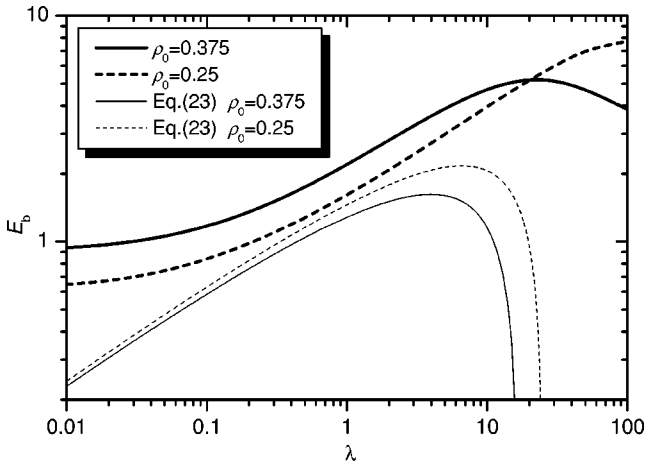

FIG. 8. Binding energy of an electron to an impurity center in a two-dimensional quantum ring as a function of the charge of the central wire. Numerical results and analytical estimates are shown. Effective atomic units are used.

Eq. (23) to weak fields. Within these conditions the agreement of the estimates and numerical results is good. This is visible for the curves $\rho_0=0.25$, which fulfill the conditions for the validity of Eq. (23) in an improved manner compared to the case $\rho_0=0.375$.

VI. SUMMARY AND CONCLUSION

We have studied analytically and numerically the problem of an impurity electron in a QR in the presence of a radially directed external electric field. The twofold character of our investigation illuminates the physical behavior and properties of our impurity-quantum ring system in a complementary way. The basis of the analytical approach is an adiabatic quasiclassical approximation, while a finite-difference method in two and three dimensions was used to perform the numerical calculations. For our analytical studies the external electric field is taken to be much stronger than the electric field due to the interaction with the impurity. The dependences of the binding energy of the impurity electron on the strength of the external electric field, the parameters of the QR, and the position of the impurity center within the QR are derived explicitly.

We have shown that if the height of the QR increases and/or the impurity center displaces from the midcircle ($z_0 \neq 0$) for any radius of the QR towards the boundary planes $z_0=\pm d/2$ of the QR, the binding energy decreases. The binding energy reaches a maximum for the impurity positioned at the midplane $z_0=0$ of the QR. For a fixed z_0 and without the radial electric field the binding energy has its maximum close to the middle point of the radial cross section of the quantum ring. The radial electric field shifts the position of the maximum towards the center of the ring in case of a positive charge of the central wire λ and in the opposite direction for a negative charge. This results in a relatively complicated dependence $E_b(\lambda)$, which is very different for different distances of the impurity from the center of the QR. The maximum value of the binding energy increases with increasing electric field strength. The amplitudes of the mentioned dependences decrease while shifting the impurity towards to the boundary planes of the QR. The inversion effect—i.e., the change of the binding energy when the direction of the electric field is changed to the opposite one—is realized in the impurity QR. Estimates of the binding energies for realistic strengths of the external electric field and the parameters of GaAs and InAs quantum rings are provided.

We have demonstrated that a strong radial electric field and ring confinement provide considerable polarization phenomena of the impurity states. Strong dependences of the binding energy of the impurity electron should lead to significant changes of transport processes and optical properties of the QR's. The great sensivity of the impurity QR's to the radial electric field is useful for its applications in field-effect transistor structures, electro-optical modulators, and switching devices.

*Electronic address: monozon@mail.gmtu.ru
†Permanent address: Institute of Precambrian Geology and Geochronology, Russian Academy of Sciences, Nab. Makarova 2, St. Petersburg 199034, Russia. Electronic address: mivanov@mi1596.spb.edu
‡Electronic address: Peter.Schmelcher@pci.uni-heidelberg.de

[1] Y. Aharonov and D. Bohm, Phys. Rev. **115**, 485 (1959).
[2] J. C. Lin and G. Y. Guo, Phys. Rev. B **65**, 035304 (2002).
[3] B. S. Monozon and P. Schmelcher, Phys. Rev. B **67**, 045203 (2003).
[4] J. M. Llorens, C. Trallero-Giner, A. Garcia-Cristobal, and A. Cantarero, Phys. Rev. B **64**, 035309 (2001).
[5] Z. Barticevic, G. Fuster, and M. Pacheco, Phys. Rev. B **65**, 193307 (2002).
[6] L. A. Lavenere-Wanderley, A. Bruno-Alfonso, and A. Latge, J. Phys.: Condens. Matter **14**, 259 (2002).
[7] P. A. Orellana, M. L. Ladron de Guevara, M. Pacheco, and A. Latge, Phys. Rev. B **68**, 195321 (2003).
[8] E. E. Mendez, G. Bastard, L. L. Chang, L. Esaki, H. Morkos, and R. Fischer, Phys. Rev. B **26**, 7101 (1982).
[9] T. Chakraborty and L. Pietiläinen, Phys. Rev. B **50**, 8460 (1994).
[10] T. Song and S. E. Ulloa, Phys. Rev. B **63**, 125302 (2001).
[11] Z. Barticevic, M. Pacheco, and A. Latge, Phys. Rev. B **62**, 6963 (2000).
[12] V. Chaplik, JETP **92**, 169 (2001).
[13] A. O. Govorov, A. V. Kalameitsev, R. Warburton, K. Karrai, and S. E. Ulloa, Physica E (Amsterdam) **13**, 297 (2002).
[14] F. Gesztesy and L. Pittner, J. Phys. A **11**, 679 (1978).
[15] *Handbook of Mathematical Functions*, edited by M. Abramowitz and I. A. Stegun (Dover, New York, 1972).
[16] H. Hasegawa and R. E. Howard, J. Phys. Chem. Solids **21**, 173 (1961).

[17] B. S. Monozon and A. G. Zhilich, Sov. Phys. JETP **73**, 1066 (1991).
[18] M. V. Ivanov, Sov. Phys. Semicond. **19**, 1167 (1985); Zh. Vychisl. Mat. Mat. Fiz. **26**, 140 (1986); J. Phys. B **27**, 4513 (1994).
[19] M. V. Ivanov, J. Phys. B **21**, 447 (1988).
[20] M. V. Ivanov and P. Schmelcher, Adv. Quantum Chem. **40** (2), 361 (2001).
[21] M. V. Ivanov, Opt. Spektrosk. **83**, 23 (1997).
[22] M. V. Ivanov and P. Schmelcher, Phys. Rev. B **65**, 205313 (2002).
[23] B. S. Monozon and A. N. Shalaginov, Solid State Commun. **89**, 167 (1994).
[24] M. V. Ivanov and R. Schinke, J. Phys.: Condens. Matter **15**, 5909 (2003).
[25] M. V. Ivanov and R. Schinke, Phys. Rev. B **69**, 165308 (2004).
[26] J. D. Jackson, *Classical Electrodynamics* (Wiley, New York, 1975).
[27] A. Fujiwara and Y. Takahashi, Nature (London) **410**, 560 (2001).